

INTERACTION BETWEEN 340 MeV π^- MESONS AND HYDROGEN

T. D. BLOKHINTSEVA, V. G. GREBINNIK, V. A. ZHUKOV, G. LIBMAN, L. L. NEMENOV, G. I. SELIVANOV, and YÜAN JUN-FANG

Joint Institute for Nuclear Research

Submitted to JETP editor August 4, 1962

J. Exptl. Theoret. Phys. (U.S.S.R.) 44, 116-126 (January, 1963)

The total cross sections of the reactions $\pi^- + p \rightarrow \pi^- + \pi^+ + n$, $\pi^- + p \rightarrow \pi^- + \pi^0 + p$, and $\pi^- + p \rightarrow \pi^- + \gamma + p$ were measured for 340 ± 15 MeV π^- -mesons with a 25 cm liquid hydrogen bubble chamber in a magnetic field. The angular distributions of the secondary particles and also the distributions of π^+ -meson production events with respect to total energy in the (π^+n) and (π^-n) c.m.s. are presented. It is shown that the effect of a resonance with a spin and isospin of $3/2$ is evident in these distributions. On the basis of an analysis of the total energy distribution in the $(\pi^+\pi^-)$ c.m.s. it is concluded that beginning with 350 MeV the cross section for $\pi\pi$ interaction in a state with a total isospin $T = 0$ rapidly increases.

INTRODUCTION

A study of the processes connected with the production of an additional meson on the nucleon in πN interaction can yield, in principle, information on the $\pi\pi$ interaction. The possibility of investigating the $\pi\pi$ interaction of inelastic collisions of pions with nucleons is noted in many papers^[1,2], where it is also emphasized that this interaction can manifest itself most clearly near the production threshold of the additional meson. The present theoretical attempts to interpret rigorously the production of mesons by mesons are represented, in particular, by the paper of Ansel'm and Gribov^[3], in which the possibility is indicated of determining the charge-exchange amplitude ($\pi^+ + \pi^- \rightarrow \pi^0 + \pi^0$) at zero energy. Experimental information pertaining to the region of near-threshold energies were obtained in many investigations carried out at primary-meson energies of 225^[4] and 245 MeV^[5]. It must be noted that the experimental investigation of this region is made extremely difficult by the very small values of the meson-production cross sections. With increasing energy, the possibility of making use of the Ansel'm and Gribov interpretation disappears, but more favorable conditions are created for the performance of the experiment.

Another way of obtaining the cross sections of the meson-meson interaction was indicated by Chew and Low^[6]. However, the use of the Chew and Low method presupposes the need of obtaining appreciable statistical material, since the errors of the result obtained upon extrapolation are very

large. In connection with the absence of a rigorous theory pertaining to energies above 250 MeV, an attempt is made in several papers^[7-10], to describe the production of the additional meson in the meson-nucleon collision either phenomenologically or on the basis of some general properties of strong interactions.

The first attempt to compare the experimental data with the predictions of the theory was made in the paper by Rodberg^[11], which was published simultaneously with the experimental investigation^[12-13] of the total cross section of the inelastic interaction of negative pions with hydrogen in the energy region from 260 to 430 MeV. It was shown that with account of $\pi\pi$ interaction it is possible to describe the variation of the cross section with energy in the entire energy interval under consideration. However, in spite of the importance of investigating the process of creation of mesons by mesons near threshold, the experimental information on the reaction $\pi^- + p \rightarrow \pi^- + \pi^+ + n$ in the energy region from 250 to 500 MeV is still scanty^[14-17], and the study of the process $\pi^- + p \rightarrow \pi^- + \pi^0 + p$ has only begun^[18,19]. It was therefore deemed interesting to obtain additional experimental material in this region of energies and to compare it with the available theoretical ideas, particularly the thorough investigation carried out by Goebel and Schnitzer^[20,21].

The possible inelastic processes at a π^- -meson energy of 340 MeV are:

$$\pi^- + p \rightarrow \pi^- + \pi^+ + n, \quad (1)$$

$$\pi^- + p \rightarrow \pi^- + \pi^0 + p, \quad (2)$$

$$\pi^- + p \rightarrow \pi^- + \gamma + p, \quad (3)$$

$$\pi^- + p \rightarrow \pi^0 + n, \quad (4)$$

$$\pi^- + p \rightarrow \pi^0 + \pi^0 + n. \quad (5)$$

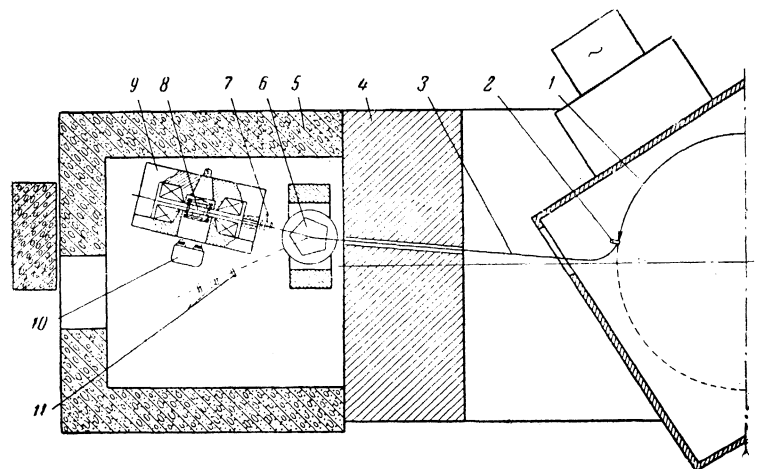
The last two reactions are extremely difficult to identify on chamber photographs and therefore are not discussed further. Exceptions are the cases in which the π^0 meson from reaction (4) decays into a gamma quantum and an electron-positron pair. The purpose of our experiment was a study of reactions (1) and (2) and (3). The investigation was carried out with a 25-cm liquid-hydrogen bubble chamber placed in a magnetic field.

1. EXPERIMENTAL CONDITIONS

The experiment was carried out in a negative-pion beam from the synchrocyclotron of the laboratory for nuclear problems of the Joint Institute for Nuclear Research. The general experimental setup is shown in Fig. 1. The beam was momentum-analyzed by the stray field of the proton synchrotron and by an additional deflecting electromagnet, and was then detected by a telescope made up of three scintillation counters. The necessary values of the deflecting-magnet field were determined by the method of the current-carrying filament^[22]. In order to separate most accurately negative pions of specified momentum, the beam was initially deflected by a 30° angle, where the maximum intensity was determined with the aid of the scintillation-counter telescope by displacing the internal target of the synchrocyclotron in radius and in azimuth. The beam was then directed to the chamber by changing the polarity of the magnet. The beam deflection angle was 10°.

The relative intensity of the particle beam at the entrance to the chamber was monitored with a second telescope of scintillation counters. The

FIG. 1. Diagram of the experiment: 1 – circulating proton beam, 2 – beryllium target, 3 – negative-pion beam, 4 – armature of synchrocyclotron magnet, 5 – concrete shield, 6 – deflecting magnet, 7 – telescope of scintillation counters, monitoring the intensity of the negative-pion beam at the entrance to the chamber, 8 – liquid-hydrogen bubble chamber, 9 – chamber magnet, 10 – stereo camera, 11 – telescope of scintillation counters, intended for preliminary separation of the monoenergetic negative-pion beam.



geometrical dimensions of the scintillators were so chosen that only those particles which were near the lower beam boundary and then did not enter the chamber passed through the scintillators.

The average number of particles entering the chamber during each expansion cycle did not exceed 10–12.

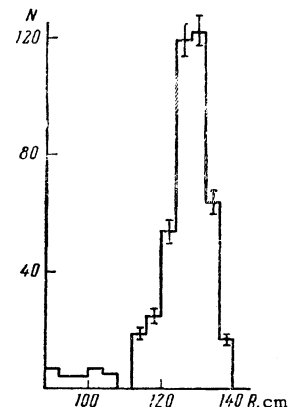
Overall control of the intensity of the internal beam of the accelerator was with the aid of an ionization chamber, and the track photography was synchronized with the beam position by a BF₃ gas-discharge counter, which registered the background of the scattered neutrons in the region of the target.

The energy spread of the particles in the beam was determined by direct measurement of the radii of curvature of the tracks on the photographs after reprojectation. The corresponding distribution, plotted on the basis of a scanning of 500 tracks, is shown in Fig. 2. The average primary negative-pion energy determined from this distribution, with account of the resolution of the method employed, was 340 ± 15 MeV.

2. LIQUID-HYDROGEN CHAMBER

The structural and technical features of the liquid-hydrogen bubble chamber used in the exper-

FIG. 2. Radius-of-curvature distribution of the tracks of the primary negative pions.



iment were reported by us in separate articles [23,24]. A diagram of the chamber is shown in Fig. 3. The value of the magnetic field in the central plane of the working volume of the chamber was 12,000 Oe. The topography of the magnetic field in the working region of the chamber, both at room temperature and at the temperature of liquid hydrogen, is shown in Fig. 4.

A correct choice of the operating conditions of the chamber influences appreciably the possibility of identifying events by the ionization density of the tracks. Therefore, in order to ensure that the production of identical track density was constant from event to event, the operating mode of the chamber was thoroughly monitored and maintained constant by several automatic stabilizing devices.

The entrance of the negative-pion beam into the chamber was through a collimator mounted in the armature of its magnet. To avoid large deflection of the beam of particles entering into the chamber, a magnetic screen was placed in the magnet gap along the direction of motion of the

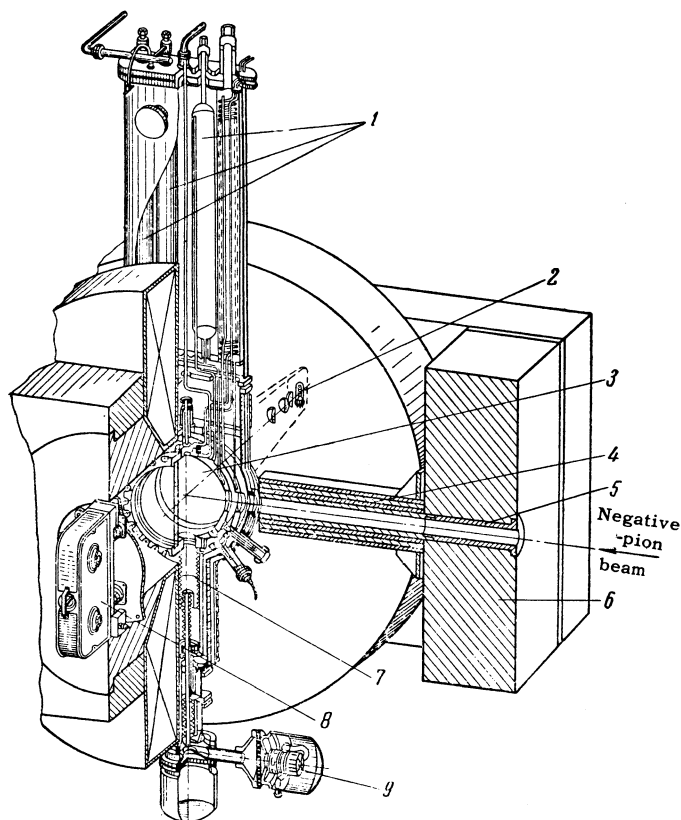


FIG. 3. Diagram of chamber: 1 – supply of liquid hydrogen, 2 – illuminator, 3 – working volume of the chamber, 4 – magnetic screen, 5 – collimator, 6 – armature of electromagnet, 7 – expansion bellows, 8 – stereo camera, 9 – electromagnetic valve.

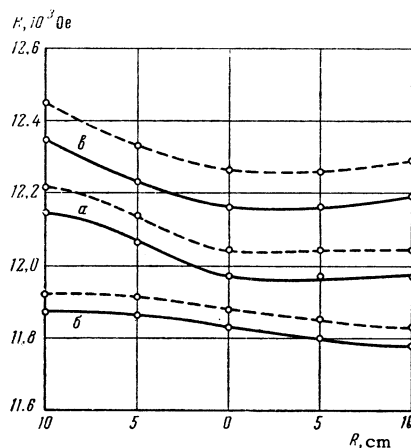


FIG. 4. Dependence of the intensity of the magnetic field in the magnet gap on the radius at room temperature (solid lines) and at the operating temperature of the chamber (dashed lines). Curves a correspond to the median plane, while curves b and c correspond to the level of the front and rear viewing windows of the chamber.

particles. The amount of wall material along the path of the entering beam was 4 g/cm^2 .

The false curvature of the tracks, due to multiple Coulomb scattering, to imperfections of the optical system, and also to the motion of the liquid in the working volume of the chamber after expansion, was measured with the aid of an automatic scanning device directly on the film, using straight tracks obtained without the magnetic field, and was found to be equal to 28 meters.

3. SCANNING OF FILMS AND SELECTION OF EVENTS

For a preliminary scanning of the events, a type 5PO-1 "Microphot" was used. All films were scanned twice by two persons. The efficiency of observing two-prong stars in a double scanning, determined from the relation $E_{12} = E_1 + E_2 - E_1 E_2$ (where E_1 and E_2 are the efficiencies of the first and second single scanings), amounted to 99.5 per cent. The processing of the frames containing double-prong stars was carried out with the aid of a reprojector, which was used to measure the following data for each event:

- 1) The angle α between the track of the entering particle and the median plane of the chamber.
- 2) The distance from the point of interaction to the edge of the visible region of the chamber.
- 3) The azimuthal angles φ_2 and φ_3 (the subscripts 2 and 3 pertain to the positive and negative particles respectively) between the median plane and the planes passing through the secondary particles and the primary track;

4) The angles θ_{12} and θ_{13} at which the secondary particles (+ and -) emerged relative to the direction of the primary track.

In choosing the necessary photographs the following criteria were employed.

1. The angle α must not exceed $\pm 4^\circ$. Such a choice of the value of α is necessitated by the fact that the negative pions hardly change their energy when deflected by an angle of 4° . This angle interval covers 93.4 per cent of the total number of particles passing through the sensitive volume of the chamber.

2. The length of the negative-pion track causing the interaction, should be not less than 10 mm. When this requirement is satisfied it becomes possible to align the images of the tracks with sufficient accuracy during the reprojection and determine the angle α .

3. The distance from the points of interaction to the edge of the visible region of the working volume of the chamber must not be less than 20 mm. This condition guarantees the possibility of measuring the momenta of the secondary particles by determining the curvature of their tracks.

4. The angle φ_3 must not exceed 70° , that is, the limit above which the accuracy of measurement with the aid of the reprojector decreases sharply.

5. The noncomplanarity of the events of elastic interaction should not go beyond $\pm 3^\circ$ and, simultaneously with it, the correlation of the angles for elastic interaction should likewise be accurate to $\pm 3^\circ$.

When the deviation from complanarity or from the calculated values of the correlation exceeded $\pm 3^\circ$, the momenta of the secondary particles were measured and compared with the values calculated from the kinematics of elastic collision, and their relative ionization was also determined.

In those cases when the measured momenta deviated from the calculated ones by more than 25 per cent, the interactions were classified as inelastic.

Reaction (1) was distinguished from reactions (2) and (3) by the angle of emission of the positive particle, by the value of its ionization, and also by

comparing the range of the positive particle, calculated from the measured momentum (assuming this particle to be a proton), with the value of the actual range, observed in the chamber. In addition, reactions (1), (2), and (3) were analyzed with the aid of the energy-conservation law, which made it possible to distinguish between reactions (2) and (3).

The reliability with which reaction (2) was distinguished from (3) is illustrated by Table I, in which are gathered all nineteen events connected with emission of a neutral particle. In the first line of the table are recorded the deviations from the energy-conservation law under the assumption that the emitted neutral particle is a π^0 meson. The figures in the second line pertain to the same cases, but under the assumption that the emitted neutral particle is a gamma quantum. In the third line are listed the proton emission angles by which it is sometimes (for $\theta_{12} > 50^\circ$) possible to identify uniquely the neutral particles as gamma quanta, taking into account the fact that at our energies the angle of emission of the proton from reaction (2) cannot exceed 50° .

Cases were classified as belonging to reaction (2) if the deviations from the energy conservation law, recorded in the first line, did not exceed one standard error in the determination of the momenta of the secondary particles, while the corresponding deviations in the second line amounted to not less than two such errors. The reactions (3) were distinguished from reactions (2) in an analogous fashion.

In those cases when the neutral pion decayed into a gamma quantum and an electron-positron pair, the reaction (4) was identified by measuring the ionizations of the secondary particles and from the value of the solid angle between them.

4. MAIN RESULTS AND CONCLUSIONS

Scanning of 16000 stereophotographs yielded 1400 two-prong stars. From among these stars, Table II lists those which satisfied the selection

Table I

Reaction	$\pi^- + p \rightarrow \pi^- + \pi^0 + p$										$\pi^- + p \rightarrow \pi^- + \gamma + p$								
	$\Delta E_{\pi^- - \pi^0}$, MeV	0	3	2	1	10	19	15	13	3	19	44	32	38	59	55	32	78	43
$\Delta E_{\pi^- - \gamma}$, MeV	32	54	42	84	70	87	99	46	48	91	124	6	18	1	9	11	13	1	3
θ_{12} , deg	22	13	27	22	10	9	38	23	38	7	13	16	16	36	44	52	37	30	60

Table II

No.	Process	Number of events	σ_{tot} , mb		Remarks
			Experiment	Theory	
1	$\pi^- + p \rightarrow \pi^- + \pi^+ + n$	108	1.24 ± 0.14	1.60	—
2	$\pi^- + p \rightarrow \pi^- + \pi^0 + p$	11	$0.13^{+0.06}_{-0.04}$	0.19	—
3	$\pi^- + p \rightarrow \pi^- + \gamma + p$	8	$0.09^{+0.03}_{-0.06}$	—	Cross section pertains to cases in which the energy of the emitted gamma quantum exceeds 100 MeV
4	$\pi^- + p \rightarrow \pi^0 + n$ $\swarrow \searrow$ $\gamma \quad e^+, e^-$	8	—	—	—
5	Elastic $\pi^- p$ scattering	764	7.52 ± 0.55	—	For negative-pion scattering angles from 30 to 150° in the laboratory system

criteria listed above. The experimental values of the total cross sections of the inelastic processes represented in the table were obtained by comparing the number of inelastic-interaction events with the number of elastic-scattering events in the l.s. negative-pion scattering-angle interval from 30 to 150°. The elastic-scattering cross section in this angle interval was obtained by integrating the angular distributions of the negative pions [25] and was found to be $\sigma_{\text{el}} = 7.52 \pm 0.55$ mb. The number of elastic events corresponding to this cross section was corrected to account for the unequal efficiency of observation of events lying in a horizontal plane and in planes close to 70°. The value of this correction in the indicated angle interval amounted to 14 per cent. For inelastic interactions this correction was insignificant and therefore was not taken into consideration.

The cross sections obtained in this manner are listed in Table II, where they are compared with the cross sections calculated by Goebel and Schnitzer [20] under the assumption that the $\pi N \rightarrow \pi\pi N$ process is described by diagrams a and b of Fig. 5. The phases of the $\pi\pi$ scattering were expressed in terms of the scattering lengths in the isotopic states 0, 1, and 2. The best agreement with the available experimental data was obtained for the following values [21] of the scattering lengths (the lower index denotes the isotopic spin):

$$\begin{aligned} a_0 &= 0.50, & a_1 &= 0.07, & a_2 &= 0.16; \\ a_0 &= 0.65, & a_1 &= 0.07, & a_2 &= -0.14, \end{aligned}$$

The agreement between the calculated cross sections and the results obtained in the present paper indicates that the parameters given above are qualitatively correct.

A comparison of the angular distributions of the neutrons from reaction (1) in the center of mass at incident pion energies of 290 [14] and 340 MeV (see Fig. 6) shows that the character of the

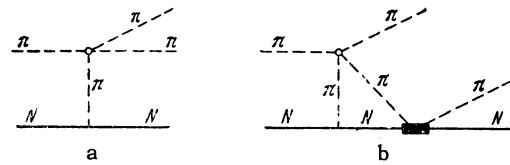


FIG. 5

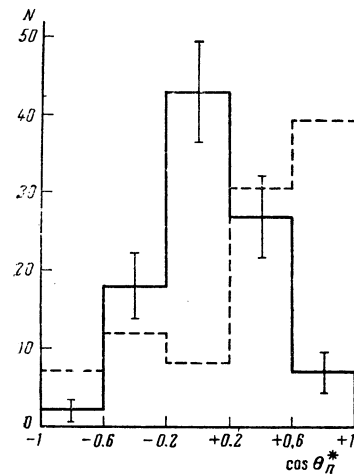


FIG. 6. Angular distributions (in the c.m.s.) of the neutrons from the reaction (1), obtained in the present work (solid line) and in the work of Batusov et al [14] (dashed line).

inelastic πN interaction changes appreciably with increasing energy of the incoming meson.

Whereas at 290 MeV the neutrons obtain large momenta and fly predominantly into the forward hemisphere, at 340 MeV they fly predominantly at angles close to 90°, which corresponds to a smaller momentum transfer to the nucleon and indicates incipient predominance of peripheral collisions which, as is well known [26], play an essential role at energies of 700–900 MeV and above.

When the kinetic energy of the incoming pions is equal to 340 MeV, the maximum permissible

total (πN) c.m.s. energy is $8.6 m_\pi c^2$. The fact that this value is close to the resonant value of the πN interaction energy, which is equal to $8.68 m_\pi c^2$, manifests itself in the momentum and energy distributions of the secondary particles. In this connection, the momentum distribution of the positive pions, which from the point of view of the isobar model^[27] are regarded predominantly as "residual," turns out to be somewhat softer than the analogous distribution of the negative pions (see Fig. 7).

In addition, from a comparison of the two histograms of Fig. 8 it can be concluded that in the ($\pi^- n$) c.m.s. the maximum permissible energies predominate, a characteristic of the isobar model.

The angular distributions of the positive and negative pions in the c.m.s. of the three final particles has the form illustrated in Fig. 9.

The distribution of the events of reaction (1) by total energy (Fig. 11) in the ($\pi^+ \pi^-$) c.m.s. is considerably shifted toward the maximum permis-

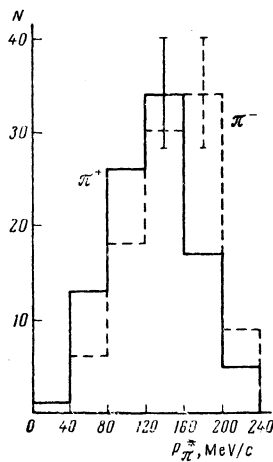


FIG. 7. Momentum distributions of positive and negative pions from the reaction (1) in the c.m.s. of the three particles.

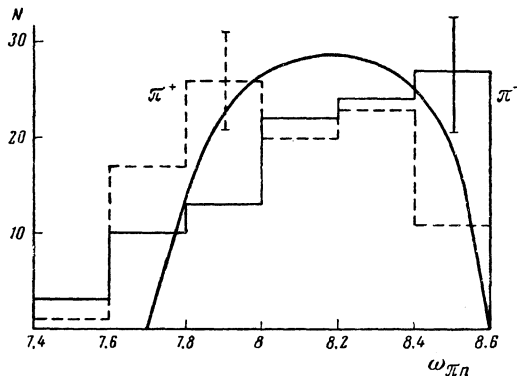


FIG. 8. Distribution by total energy (in $m_\pi c^2$ units) ($\pi^+ n$) and ($\pi^- n$) c.m.s. in the case of reaction (1).

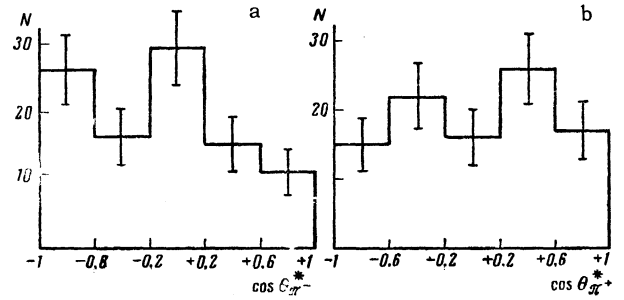


FIG. 9. Angular distributions of π^+ mesons (a) and π^- mesons (b) in the c.m.s. of the three final particles.

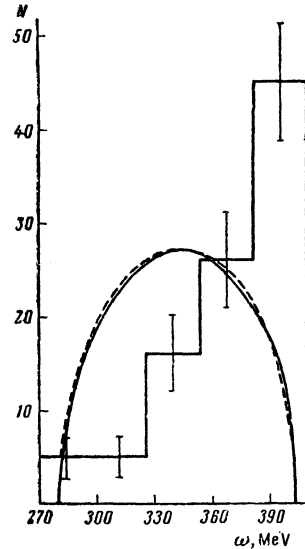


FIG. 10. Distribution by total energy in the ($\pi^+ \pi^-$) c.m.s. for the case of reaction (1). The solid line denotes the phase volume calculated from the statistical theory, while the dashed line the volume obtained from the isobar model.

sible energies and is not described by curves calculated from the statistical theory and the isobar model.

In this connection, it is advantageous to compare the result obtained with the results of Kirz, Schwartz, and Tripp^[28], who investigated the reaction $\pi^+ + p \rightarrow \pi^+ + \pi^+ + n$ and found that the momentum distribution in the c.m.s. of the two pions is in good agreement with the phase-volume curve. It follows therefore that the matrix element describing the $\pi\pi$ interaction in the state with total isotopic spin, $T = 2$ remains practically constant in the indicated energy interval, and thus cannot cause a sharp deviation from the calculated curves observed in our experiment. It is therefore necessary to assume that the displacement observed in the ($\pi^+ \pi^-$) c.m.s. toward the maximum energies is due to $\pi\pi$ interaction in the states with $T = 0$ and $T = 1$.

By making use of the data of^[29], obtained for experiments on pair production of mesons in pd collisions at approximately the same energy in the two-pion c.m.s., we get more information on the contribution of the states with $T = 0$ and $T = 1$. It was shown in these experiments that the cross section for the production of two pions in a state with isotopic spin $T = 1$ is small and in the energy region under consideration remains practically constant, whereas the cross section for the production of two pions in the state with $T = 0$ increases rapidly with energy. It is therefore natural to conclude that the observed rise in the distribution by the total energy in the c.m.s. of the two pions is due to their interaction in the state $T = 0$. An analogous deduction concerning the character of the interaction in the $\pi^+\pi^-$ system is made also by Schwartz, Kirz, and Tripp^[16], who worked with a primary-meson energy of 350 MeV.

In conclusion, the authors consider it their pleasant duty to thank Prof. B. M. Pontecorvo for continuous interest in the work and for valuable advice, and P. F. Ermolova for useful discussions. We are also grateful to N. Antonova, N. Kurilina, and I. Shevchenko for much labor in scanning and processing the films.

¹G. F. Chew, Paper at the International Conference on High-energy Particles, Kiev, (1959).

²B. M. Pontecorvo, *ibid.*

³A. A. Ansel'm and V. N. Gribov, JETP 37, 501 (1959), Soviet Phys. JETP 10, 354 (1960).

⁴Deahl, Derrick, Fetkovich, Fields, and Yodh. Proceedings of the International Conference on High-energy Physics, Rochester (1960), p. 185.

⁵Batusov, Bunyatov, Sidorov, and Yarba, JETP 39, 1850 (1960), Soviet Phys. JETP 12, 1290 (1961).

⁶G. F. Chew and F. L. Low, Phys. Rev. 113, 1640 (1959).

⁷S. Barshaw, Phys. Rev. 111, 1651 (1958).

⁸R. F. Peierls, Phys. Rev. 111, 1373 (1958).

⁹V. V. Anisevich, JETP 39, 97 (1960), Soviet Phys. JETP 12, 71 (1961).

¹⁰K. S. Marish, Preprint, Joint Inst. Nuc. Res. D-793 (1961).

¹¹L. S. Rodberg, Phys. Rev. Lett. 3, 58 (1959).

¹²V. G. Zinov and S. M. Korenchenko, JETP 38, 1099 (1960), Soviet Phys. JETP 11, 794 (1960).

¹³Perkins, Caris, Keuney, Knapp, and Perez-Mendez, Phys. Rev. Lett. 3, 56 (1959).

¹⁴Batusov, Bunyatov, Sidorov, and Yarba, JETP 40, 460 (1961), Soviet Phys. JETP 13, 1320 (1961).

¹⁵Barish, Kurz, McManigal, Perez-Mendez, and Solomon, Phys. Rev. Lett. 6, 297 (1961).

¹⁶Schwartz, Kirz, and Tripp, Bull. Amer. Phys. Soc. 7, 282 (1962).

¹⁷Barish, Kurz, Perez-Mendez, and Solomon, Bull. Amer. Phys. Soc. 6, 523 (1961).

¹⁸Batusov, Bunyatov, Sidorov, and Yarba, JETP 40, 1528 (1961), Soviet Phys. JETP 13, 1070 (1961).

¹⁹Goodwin, Kenney, and Perez-Mendez, Phys. Rev. 122, 655 (1961).

²⁰J. J. Goebel and H. J. Schnitzer, Phys. Rev. 123, 1021 (1961).

²¹H. J. Schnitzer, Phys. Rev. 125, 1059 (1959).

²²M. S. Kozodaev and A. A. Tyapkin, PTÉ, No 1, 21 (1956).

²³Blokhintseva, Vasilenko, Grebinnik, Zhukov, Libman, Nemenov, Selivanov and Yüan, PTÉ, No 5, 51 (1962).

²⁴Balandin, Grebinnik, and Selivanov, PTÉ, No 5, 60 (1962).

²⁵S. M. Korenchenko, Dissertation, Joint Inst. Nuc. Res. (1959).

²⁶A. Pickup, Phys. Rev. Lett. 7, 192 (1961).

²⁷R. M. Sternheimer and S. J. Lindenbaum, Phys. Rev. 109, 1723 (1958).

²⁸Kirz, Schwartz, and Tripp, Preprint UCRL-9941 (1961).

²⁹Akimov, Komarov, Marish, Savchenko, and Soroko, JETP 40, 1532 (1961), Soviet Phys. JETP 13, 1073 (1961).

Translated by J. G. Adashko